

Article

Not peer-reviewed version

---

# In Silico and In Vivo Evaluation of Novel 2-Aminobenzothiazole Derivative Compounds as Antidiabetic Agents

---

[Juan Andres Alvarado Salazar](#)\*, [Miguel Valdes](#)\*, [Alejandro Cruz](#), Brenda Moreno De Jesús, [David Patiño González](#), [Ivonne María Olivares-Corichi](#), [Feliciano Tamay Cach](#), [Jessica Elena Mendieta Wejebe](#)\*

Posted Date: 30 August 2024

doi: 10.20944/preprints202408.2205.v1

Keywords: 2-aminobenzotiazol; isotioureas; guanidinas; diabetes tipo 2; actividad antidiabética



Preprints.org is a free multidiscipline platform providing preprint service that is dedicated to making early versions of research outputs permanently available and citable. Preprints posted at Preprints.org appear in Web of Science, Crossref, Google Scholar, Scilit, Europe PMC.

Copyright: This is an open access article distributed under the Creative Commons Attribution License which permits unrestricted use, distribution, and reproduction in any medium, provided the original work is properly cited.

Article

# In Silico and In Vivo Evaluation of Novel 2-Aminobenzothiazole Derivative Compounds as Antidiabetic Agents

Andres Alvarado Salazar <sup>1,\*</sup>, Miguel Valdes <sup>2,\*</sup>, Alejandro Cruz <sup>3</sup>, Brenda Moreno de Jesús <sup>2</sup>, David Patiño González <sup>2</sup>, Ivonne María Olivares Corichi <sup>4</sup>, Feliciano Tamay Cach <sup>5</sup> and Jessica Elena Mendieta Wejebe <sup>2,\*</sup>

<sup>1</sup> Carrera de Química Farmacéutica Biológica, Área Farmacéutica, Facultad de Estudios Superiores (FES)-Zaragoza, Universidad Nacional Autónoma de México, Batalla 5 de mayo s/n, Ejercito de Oriente, Iztapalapa, Ciudad de México 09230, México

<sup>2</sup> Laboratorio de Biofísica y Biocatálisis, Sección de Estudios de Posgrado e investigación, Escuela Superior de Medicina, Instituto Politécnico Nacional, Av. Salvador Díaz Mirón esq. Plan de San Luis s/n, Casco de Santo Tomás, Miguel Hidalgo, Ciudad de México 11340, México

<sup>3</sup> Laboratorio de Química Supramolecular y Nanociencias, Departamento de Ciencias Básicas, Unidad Profesional Interdisciplinaria de Biotecnología, Instituto Politécnico Nacional, Av. Acueducto s/n, Colonia Barrio La Laguna Ticomán, Ciudad de México 07340, México

<sup>4</sup> Laboratorio de Bioquímica y Estrés Oxidante, Sección de Estudios de Posgrado e investigación, Escuela Superior de Medicina, Instituto Politécnico Nacional, Av. Salvador Díaz Mirón esq. Plan de San Luis s/n, Casco de Santo Tomás, Miguel Hidalgo, Ciudad de México 11340, México

<sup>5</sup> Laboratorio de Investigación de Bioquímica Aplicada, Sección de Estudios de Posgrado e investigación, Escuela Superior de Medicina, Instituto Politécnico Nacional, Av. Salvador Díaz Mirón esq. Plan de San Luis s/n, Casco de Santo Tomás, Miguel Hidalgo, Ciudad de México 11340, México

\* Correspondence: alvarado.salazar.ja@gmail.com (A.A.S.); valdesguevaramiguel@gmail.com (M.V.); jesmenwej@yahoo.com (J.E.M.W.)

**Abstract:** Currently, there are several drugs used for the treatment of type 2 diabetes (T2D), however, all of them have adverse effects. Benzothiazoles have a broad spectrum of biological activities such as antidiabetic. This study aimed to evaluate in silico and in vivo two series of 2-aminobenzothiazole derivatives linked to isothiourreas (**3a-w**) or guanidines (**4a-z**) for the treatment of T2D. The ADMET properties were determined in silico from which it was possible to select compounds **3a**, **3b**, **4a**, **4b**, **4c**, **4r**, **4s**, **4x**, and **4y** and, with molecular docking, it was shown that **3b** and **4y** showed high affinity for PPAR gamma ( $\Delta G = -7.8$  and  $-8.4$  kcal/mol, respectively). In vivo, the LD<sub>50</sub> value was estimated in rat based on OECD Guideline 425, being  $> 1750$  mg/kg for both compounds. The pharmacological effect of **3b** and **4y** was evaluated in the T2D rat model, showing that after oral administration in equimolar ratio to pioglitazone (15 mg/kg) for 4 weeks, both compounds were able to reduce blood glucose levels ( $< 200$  mg/dL) and improve the lipid profile. Therefore, **3b** and **4y** could be used in the future as antidiabetic agents.

**Keywords:** 2-aminobenzothiazole; isothiourreas; guanidines; type 2 diabetes; antidiabetic activity

## 1. Introduction

Diabetes is a chronic and progressive endocrine disease characterized by uncontrolled hyperglycemia, which is associated with poor pancreatic function in the synthesis and secretion of insulin and an inadequate response of peripheral tissues to the action of this hormone, which leads to a series of metabolic alterations that cause cellular dysfunction [1]. Over time, these pathological processes lead to the development of complications that can cause serious health problems [2–9]. In 2021, the global prevalence of people aged 20 to 79 years diagnosed with diabetes was estimated at

10.5% (536.6 million) and is expected to increase to 12.2% (783.2 million) by 2045 [10]. It is known that in low- and middle-income countries there is a higher prevalence and mortality of people with diabetes [10–12].

Because most patients with diabetes have type 2 diabetes (T2D), this disease has become a challenge for the scientific community [13]. Pharmacological therapies available for the treatment of T2D include oral hypoglycemic agents, the most used being biguanides, sulfonylureas, thiazolidinediones, and alpha-glucosidase inhibitors. Other therapies include glucagon-like peptide-1 agonists, dipeptidyl peptidase-4 inhibitors, sodium-glucose cotransporter-2 inhibitors, and insulin [4,14–17]. These drugs can be administered as monotherapy, but considering that T2D is a progressive disease, its management in more advanced stages requires the combination of several oral hypoglycemic agents to maintain the efficacy of the treatment [18]. However, this leads to an increasing profile of side effects in which the incidence or severity of damage to health will depend on each of them, which ultimately becomes a limiting factor of the treatment [19]. Therefore, there is a need to search for alternative therapeutic agents for the treatment of T2D, which are based on the use of structural prototypes for the development of new chemical entities with potential antidiabetic activity [6,20]. In this regard, it has been reported that various compounds incorporating heterocyclic and fused heterocyclic rings play an important role in the design and synthesis of antidiabetic agents, mainly those containing nitrogen, sulfur and oxygen atoms have attracted medical interest due to their countless and promising pharmaceutical applications [21,22].

Benzothiazoles are compounds belonging to the class of bicyclic heteroaromatics, which have shown a broad spectrum of biological activities, such as antimicrobial, anticancer and antidiabetic, among others [23–27]. There are several commercially available drugs that contain the benzothiazole nucleus, such as etoxzolamide, which is used in heart diseases, glaucoma and more recently as an antimicrobial agent [28–31]. Among the derivatives of the 2-aminobenzothiazole nucleus is riluzole, which is useful in the treatment of amyotrophic lateral sclerosis [32,33], while frentizole has antiviral and immunosuppressive properties [22,34], although its pharmacological effect has also been identified in neurodegenerative disorders [35–37]. On the other hand, zopolrestat was developed by Pfizer for the treatment of diabetic complications [21,38]. In this regard, several studies have shown that the antidiabetic activity of different series of compounds derived from the benzothiazole nucleus is associated with their agonist effect on the peroxisome proliferator-activated receptor gamma (PPAR gamma) [23,39–43].

Therefore, this study aimed to evaluate the antidiabetic activity of hybrid compounds derived from the 2-aminobenzothiazole nucleus linked to different isothioureas (**3a-w**) or guanidines (**4a-z**) (Figure 1) in a rat model with T2D, which were previously designed and synthesized by our research group [44–49].

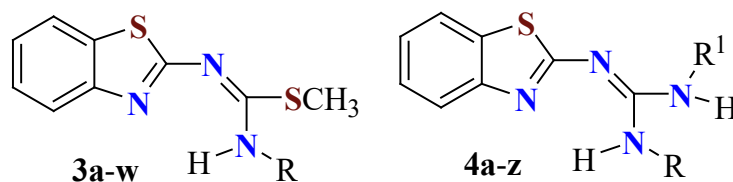


**Figure 1.** General chemical structure of 2-aminobenzothiazole derivatives linked to different isothioureas (**3a-w**) or guanidines (**4a-z**).

## 2. Results and Discussion

### 2.1. *In Silico* Studies

#### 2.1.1. ADMET Properties

Forty-nine molecules derived from the 2-aminobenzothiazole nucleus linked to isothioureas (**3a-w**) or guanidines (**4a-z**) were designed (Figure 1). Subsequently, their physicochemical properties and toxicity parameters were determined, which allowed the first screening to be carried out,

obtaining a total of 28 compounds. The second screening was carried out by calculating the parameters of aqueous solubility, pharmacokinetics and medicinal chemistry. Finally, the third screening was carried out considering the value of the free binding energy ( $\Delta G$ ) obtained from the molecular docking, with which 9 compounds with very high potential for the treatment of T2D were chosen. The results obtained from this first in silico study are presented below, considering the data from the 9 compounds chosen as the most promising up to that point (Tables 1-4). The way in which the score was assigned in each screening from the 49 compounds is described in the Supplementary Materials (Tables 2S-4S).

**Table 1.** Compounds benzothiazolisothiureas (3) and guanidinobenzothiazoles (4) with the highest score obtained from the values of their physicochemical, pharmacological and toxicological properties by online servers.

Compound	Chemical structure
3a	
3b	
4a	
4b	
4c	
4r	
4s	
4x	
4y	

Abbreviations: 3a: N'-(1,3-benzothiazol-2-yl)(methylsulfanyl)metanimidamide; 3b: N'-(1,3-benzothiazol-2-yl)-N-methyl(methylsulfanyl)metanimidamide; 4a: N'-(1,3-benzothiazol-2-yl)guanidine; 4b: N'-(1,3-benzothiazol-2-yl)-N-methylguanidine; 4c: N'-(1,3-benzothiazol-2-yl)-N,N'-dimethylguanidine; 4r: N-(1,3-benzothiazol-2-yl)-2,3-dihydro-1,3-benzoxazol-2-imine; 4s: N-(2,3-dihydro-1H-1,3-benzodiazole-2-ylidene)-1,3-benzothiazol-2-amine; 4x: N'-(1,3-benzothiazol-2-yl)-N,N'-bis(propan-2-yl)guanidine; 4y: N'-(1,3-benzothiazol-2-yl)-N,N'-di-tert-butylguanidine.

The physicochemical properties and toxicity parameters of the evaluated compounds are presented in Table 2. This set of data is known as Lipinski and Veber rules [50–52], which must be fulfilled by new chemical entities to be considered as potential oral drugs. The molecular weight (MW) should be less than 500 g/mol, the water-octanol partition coefficient (cLogP) should be less than 5, which indicates that it has adequate liposolubility through the cell membrane, it should not have more than 10 acceptors (nON) or more than 5 donors (nOHNH) of hydrogen bonds, the number

of rotatable angles (nrotb) should be less than 10 and the topological polar surface area (TPSA) should be less than 140 Å<sup>2</sup>, since it represents adequate permeability in cells of the digestive tract, while if the value is less than 90 Å<sup>2</sup>, a good penetration of the blood-brain barrier (BBB) can be assumed [50–55].

**Table 2.** Physicochemical properties and toxicity parameters of the best benzothiazolisothioureas (3) and guanidinobenzothiazoles (4) compounds obtained from Molinspiration Cheminformatics and DataWarrior.

Compound	Physicochemical properties					Toxicity (DW)				ODLS	
	MW (g/mol)	cLogP	nON	nOHNH	nrotb	TPSA (Å <sup>2</sup> )	M	T	IE		RE
3a	223.33	2.41	3	2	2	51.28	X	X	X	X	1.0
3b	237.35	2.79	3	1	3	37.28	X	X	X	X	1.0
4a	192.25	2.29	4	4	1	77.30	X	X	X	X	1.0
4b	206.27	2.67	4	3	2	63.31	X	X	X	X	1.0
4c	220.30	3.04	4	2	3	49.31	X	X	X	X	1.0
4r	267.31	4.14	4	1	1	54.19	X	X	X	X	1.0
4s	266.33	4.04	4	2	1	56.84	X	X	X	X	1.0
4x	276.41	4.38	4	2	5	49.31	X	X	X	X	1.0
4y	304.46	5.41	4	2	5	49.31	X	X	X	X	0.92
PGZ	356.45	3.07	5	1	7	68.30	X	X	X	X	1.0

Abbreviations: PGZ: pioglitazone; DW: DataWarrior; MW: molecular weight; cLogP: octanol-water partition coefficient; nON: number of hydrogen bond acceptors; nOHNH: number of hydrogen bond donors; nrotb: number of rotatable bonds; TPSA: topological polar surface area; M: mutagenicity; T: tumorigenicity; IE: irritant effects; RE: reproductive effects; ODLS: overall drug-likeness score. √: it does present the effect; X: it does not present the effect.

As can be observed in Table 2, most of the compounds satisfactorily comply with Lipinski's rule of five [50,51] and the considerations of Veber et al. [52], except for 4y, which has a cLogP value greater than 5, which is not very advisable considering that this parameter is associated with hydrophobicity that affects drug absorption, bioavailability, hydrophobic ligand-protein interactions, metabolism of the compounds, as well as their toxicity. However, 4y was not discarded from this first virtual screening even though it would be advisable to make some structural modifications to this compound in the future. In addition, according to the predictors used, it is suggested that none of the evaluated compounds is associated with mutagenicity, tumorigenicity and/or irritant and reproductive effects. Based on these results, in the last column of Table 2 it is possible to observe the value of the overall drug similarity score (ODLS), which qualitatively evaluates the possibility of a compound becoming an orally administered drug with respect to its bioavailability [52].

Subsequently, the compounds with a ODLS of 1.0 were determined for their toxicological properties using Tox-Prediction, which are presented in Table 3. The results show that all compounds belong to Class IV (300 < LD50 ≤ 2000 mg/kg), indicating that they produce low toxicity according to the Globally Harmonized System of Classification and Labeling of Chemicals [56]. Therefore, since the LD50 value is high (> 1750 mg/kg), the compounds are expected to be quite safe for use as pharmaceuticals.

**Table 3.** Toxicological properties of the best benzothiazolisothioureas (3) and guanidinobenzothiazoles (4) compounds obtained from Tox-Prediction.

Compound	LD50 (mg/kg)	Class	Hepatotoxicity	Immunotoxicity	Citotoxicity
3a	1190	IV	X	X	X

<b>3b</b>	1000	IV	X	X	X
<b>4a</b>	1190	IV	X	X	X
<b>4b</b>	1190	IV	X	X	X
<b>4c</b>	1190	IV	X	X	X
<b>4r</b>	1190	IV	X	X	X
<b>4s</b>	1190	IV	X	X	X
<b>4x</b>	1190	IV	X	X	X
<b>4y</b>	1190	IV	X	X	X
PGZ	1000	IV	X	X	X

Abbreviations: PGZ: pioglitazone; LD50: median lethal dose. X: it does not present the toxicological effect.

Table 4 presents the aqueous solubility, pharmacokinetic and medicinal chemistry parameters of the compounds analyzed in SwissADME. Aqueous solubility is a characteristic of great pharmaceutical importance for compounds proposed as potential enteral medications, since this property facilitates the handling and formulation of these compounds, and also influences their intestinal absorption. In this regard, the compound considered highly soluble in aqueous medium (Class IV) is **4a**, while the moderately soluble (Class II) are **4r** and **4s**. The rest of the evaluated compounds present a medium solubility (Class III).

**Table 4.** Aqueous solubility, pharmacokinetics and medicinal chemistry parameters of the best benzothiazolisothioureas (**3**) and guanidinobenzothiazoles (**4**) compounds obtained from SwissADME.

Compound	Aqueous solubility			Pharmacokinetics								OD		
	logS	Solubility (mg/mL)	Class	GI	BBB	P-gp	CYP450 inhibitor						BD	LS
							1A2	2C19	2C9	2D6	3A4			
<b>3a</b>	-3.00	2.24e-01	III	√	X	X	√	√	X	X	X	0.55	0.84	
<b>3b</b>	-3.24	1.37e-01	III	√	X	X	√	√	√	X	X	0.55	0.80	
<b>4a</b>	-1.95	2.15e+00	IV	√	X	X	√	X	X	X	X	0.55	0.92	
<b>4b</b>	-2.19	1.34e+00	III	√	X	X	√	X	X	X	X	0.55	0.88	
<b>4c</b>	-2.43	8.22e-01	III	√	X	X	√	X	X	X	X	0.55	0.88	
<b>4r</b>	-4.51	8.31e-03	II	√	X	X	√	X	X	X	X	0.55	0.84	
<b>4s</b>	-4.14	1.95e-02	II	√	X	X	√	X	X	X	√	0.55	0.80	
<b>4x</b>	-3.56	7.64e-02	III	√	√	X	√	√	√	X	X	0.55	0.80	
<b>4y</b>	-3.93	3.56e-02	III	√	X	X	√	√	√	X	X	0.55	0.80	
PGZ	-4.31	1.76e-02	II	√	X	X	√	√	√	√	√	0.55	0.68	

Compound	Drug-likeness					Medicinal chemistry		
	Lipins ki	Ghose	Veber	Egan	Muegge	PAINS	Brenk	Synthesis accesibility
<b>3a</b>	√	√	√	√	√	0	2	2.83
<b>3b</b>	√	√	√	√	√	0	2	3.03
<b>4a</b>	√	√	√	√	X	0	2	2.50
<b>4b</b>	√	√	√	√	√	0	2	2.69
<b>4c</b>	√	√	√	√	√	0	2	2.77
<b>4r</b>	√	√	√	√	√	0	0	3.22
<b>4s</b>	√	√	√	√	√	0	0	2.86
<b>4x</b>	√	√	√	√	√	0	2	3.16
<b>4y</b>	√	√	√	√	√	0	2	3.38
PGZ	√	√	√	√	√	0	1	3.46

Abbreviations: logS: logarithm of the aqueous solubility; Class: V (highly soluble), IV (very soluble), III (soluble), II (moderately soluble), I (poorly soluble); GI: gastrointestinal absorption (√: high, X: low); BBB: blood-brain barrier permeability; P-gp: P-glycoprotein substrate; CYP450: cytochrome P-450; BD: bioavailability. √: it does

present activity; X: it does not present activity. Lipinski's rule of five (Pfizer), Ghose filter, Veber filter, Egan filter (Pharmacia), Muegge filter (Bayer):  $\checkmark$ : it meets all parameters, X: it does not meet all parameters; PAINS: interference structures in panel assays (structures that may present a false positive in activity); Brenk: structural alert; synthesis accessibility: 1 easy-10 difficult.

On the other hand, all compounds show a high gastrointestinal (GI) absorption, indicating that they are susceptible to the first-pass effect, while the only compound that is able to cross the BBB is **4x**. Within the pharmacokinetic parameters, it is of great value to know whether or not a compound is a substrate of P-glycoprotein (P-gp), which is the most important in the function of ATP-dependent transporters (ABC), since it stands out for its multiple functions in the digestive tract, in the central nervous system and also because it is overexpressed in different types of cancer leading to resistance to multiple drugs [57,58]. In the case of the compounds presented in Table 4, it is predicted that none of them is a substrate of P-gp. Similarly, it is essential to understand the interaction of xenobiotics with cytochrome P450 (CYP450), which is the main superfamily of isoenzymes responsible for the elimination of drugs through their biotransformation into water-soluble (polar) compounds. However, the inhibition of one or more CYP450 isoenzymes is related to various drugs that have toxic effects and lead to adverse effects. According to Di and Wolf et al., 50 to 90% of drugs interact with five main human CYP450 isoforms (1A2, 2C19, 2C9, 2D6, 3A4) and the inhibition of any of these leads to adverse effects due to toxicity [59]. Therefore, it is of great importance to highlight that none of the compounds evaluated inhibits all CYP450 isoforms, unlike drugs such as pioglitazone (PGZ) which, by inhibiting the five CYP450 isoforms, has been shown to cause ventricular hypertrophy and hepatic and renal congestion in Swiss albino mice [60].

In addition to using pharmacokinetic and toxicological parameters and Lipinski's rule of five [50,51], major pharmaceutical companies have established various filters to have reliable and high-quality chemical compound libraries. In this sense, the improvements that have been made to Lipinski's rule of five were published in 1999 as the Ghose rules (Amgen Inc.), which establish that the cLogP value must be between -0.4 and +5.6, the MW must be greater than 160 and less than 500 g/mol, the molar refractivity must have a value between 40 and 130 and the total number of atoms must be between 20 and 70. For its part, Veber's rules [52] indicate that molecules must have an TPSA value less than 140 Å<sup>2</sup> and the nrotb must be less than 10. Egan's rules established by the pharmaceutical and biotechnology company Pharmacia, establish that the allowed TPSA value must be less than 136.1 Å<sup>2</sup> and the cLogP less than 5.88 to consider a chemical entity as a potential drug. Muegge's rules state that the MW must be greater than 200 and less than 600 g/mol, the cLogP value must be between -2 and 5, the TPSA must be less than 150 Å<sup>2</sup>, the number of rings in a structure must be less than 7, the number of carbon atoms must be greater than 5 and the number of heteroatoms greater than 1, it must not have more than 15 nrotb, the hydrogen acceptors and donors that can form hydrogen bonds must not exceed 10 and 5, respectively. In Table 4, it can be observed that most of the molecules do not violate the Lipinski's rule of five (Pfizer), Ghose, Veber, Egan and Muegge, except for molecule **4a** which violates one of Muegge's rules by having a molecular weight less than 200 g/mol.

In the medicinal chemistry section, several aspects are considered, the PAINS are promiscuous structures that can have biological activity against various molecular targets independently of the pharmacological target, while the Brenk parameters include a list of 105 fragments that could cause toxicity, in addition to being associated with poor pharmacokinetic properties, poor metabolism and high chemical reactivity. This information guides us to a possible chemical modification with the aim of increasing pharmacological activity and decreasing or avoiding undesired effects. Likewise, a factor of great importance in drug design is the chemical synthesis process, therefore, the prediction of a high success rate in obtaining synthetic compounds is classified as 1 easy and 10 difficult in terms of synthesis. In this sense, it can be observed in Table 4 that the synthesis accessibility scores of the proposed compounds are in a range of 2 to 4, which confirms what was previously reported in that they are relatively easy to obtain [44–49].

In summary, in the first screening, which started with 49 compounds, those with a ODLs of 1.0 were selected. Subsequently, with the evaluation of aqueous solubility, pharmacokinetics and

medicinal chemistry, it was possible to choose the compounds that obtained a ODLS equal to or greater than 8.0. To select the compounds that would go on to the next screening, Tables 2-4 were compared in order to verify that all of them contained the highest scoring compounds to be evaluated in the next phase of the in silico study, which corresponds to molecular docking.

### 2.1.2. Molecular Docking

Molecular docking analysis was performed by evaluating the interactions of each of the ligands selected in the third screening (**3a**, **3b**, **4a**, **4b**, **4c**, **4r**, **4s**, **4x**, and **4y**) with PPAR gamma, which was one of the most similar molecular targets according to the reverse docking previously performed in DIA-DB (data not shown). The  $\Delta G$  values that were obtained for the 9 best ligands range from -6.4 to -8.4 kcal/mol (Table 5S), being among the most promising compounds of the benzothiazolisothiureas and guanidinobenzothiazoles series **3b** ( $\Delta G = -7.8$  kcal/mol) and **4y** ( $\Delta G = -8.4$  kcal/mol), respectively. It is worth mentioning that, although most of the  $\Delta G$  values of the evaluated ligands do not exceed the  $\Delta G$  value of the reference ligand (PGZ,  $\Delta G = -9.5$  kcal/mol), most of them present acceptable values ( $> -7.0$  kcal/mol). Figure 2 presents the binding mode and type of interactions between ligands **3b** and **4y** with PPAR gamma, considering that they were among the best qualified according to their respective  $\Delta G$  values. However, the interactions of the remaining 7 ligands with the protein of interest were also analyzed, finding similar results (data not shown).

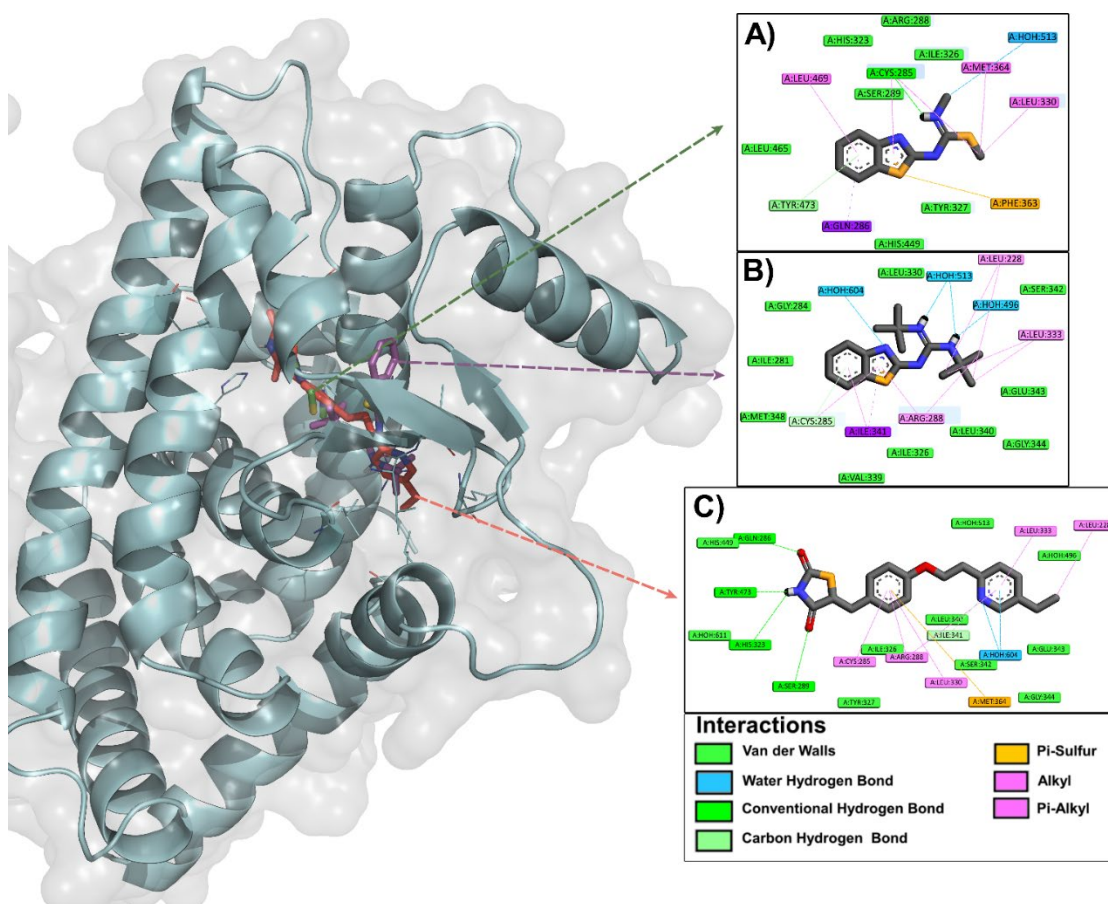


**Figure 2.** Binding mode and type of interactions presented between ligands **3b** (A), **4y** (B), and PGZ (C) with PPAR gamma.

Several studies have identified the forms of interaction of full and partial agonists with PPAR gamma, which is made up of a Y-shaped ligand binding domain (LBD) consisting of arms I, II, and III. Arm I extends towards helix 12 (H12) and is characterized by being polar and widely conserved in the three PPAR subtypes (alpha, beta/delta, and gamma). It is linked to the activator function 2 (AF-2) in the C-terminal region that maintains its active conformation through a network of hydrogen

bonds with arm I, which favors ligand binding. Arms II and III are less conserved than arm I among PPAR subtypes and both are hydrophobic in nature [61–64]. It has been proposed that several ligands bind to the PPAR gamma LBD through a hydrophilic interaction with the arm I region and hydrophobic interactions with regions of arms II or III. Partial agonists activate PPAR gamma through a mechanism independent of the H12 conformational change induced by full agonists, since most have been shown to occupy regions of arms II and III between helix 3 (H3) and the beta sheet, leading to a decrease in H12 stability that affects coactivator binding and, consequently, PPAR gamma transcriptional activity [61]. Furthermore, the key residues in the LBD that induce receptor activation in the presence of a partial agonist are completely different from those that induce activation in the presence of a full agonist, since almost all partial agonists can stabilize the beta sheet through hydrogen bonding of an acidic group with the amine of the Ser342 backbone. However, partial agonists lacking an acidic group can also stabilize the beta-sheet through hydrophobic interactions, especially with the side chain of Ile341. Furthermore, most partial agonists interact hydrophobically with Cys285 of H3 and with Arg288 through electrostatic interactions or hydrophobic or van der Waals interactions. Partial agonists extending into arm I of the LBD only form a hydrogen bond with one of the AF2 residues and make electrostatic interactions with other residues in proximity such as Tyr327 or Ser289, although they can also form limited hydrophobic interactions with H12, such as with Leu469. Finally, some partial agonists form other interactions at the edges of the LBD, including pi-pi interactions with Phe282 of helices H3, Phe264 of the loop adjacent to H2' and Phe363 of helix H7 [61–64]. Figure 2 shows that the most representative interacting residues are Tyr327, Ser289, Leu469, Cys285, Arg288, Phe282, and Phe363 for compound **3b**, while for **4y** they are Tyr327, Ser289, Cys285, Arg288, Ile341 and Phe363.

In summary, the selection of the best compounds to continue with further studies was carried out based on the score obtained in the prediction of the ADMET properties. However, the  $\Delta G$  value and the type of ligand-protein interactions obtained from the molecular docking study were decisive in defining the candidates to be evaluated in vivo.

## 2.2. In Vivo Studies

### 2.2.1. Acute Oral Toxicity Test (AOT) of Compounds **3b** and **4y**

In Table 5 it can be observed that the administration of compounds **3b** and **4y** did not cause the death of animals at any of the doses evaluated (175, 550, and 1750 mg/kg) based on the Guide No. 425 of the Organisation for Economic Co-operation and Development for the evaluation of AOT [65], so the value of the median lethal dose (LD50) is greater than 1750 mg/kg in both cases. These results show that compounds **3b** and **4y** belong to Class IV according to the GHS, indicating that they have low toxicity thus may be safe for their pharmaceutical use. [56].

**Table 5.** Data from the AOT test performed with compounds **3b** and **4y**.

Compound <b>3b</b>			
Doses (mg/kg)	Mortality rate (%)	LD50 (mg/kg)	GHS category
175	0		
550	0	> 1750	Clase IV
1750	0		
Compound <b>4y</b>			
Doses (mg/kg)	Mortality rate (%)	LD50 (mg/kg)	GHS category
175	0		
550	0	> 1750	Clase IV
1750	0		

Abbreviations: LD50: median lethal dose; GHS: Globally Harmonized System of Classification and Labeling of Chemicals.

Figure 3 shows the photographs corresponding to the necropsy performed 15 days after the animals were administered compounds **3b** and **4y**. As can be seen, neither of the two compounds produced obvious macroscopic damage to the organs and tissues of the animals, which presented normal characteristics in terms of size and color (Figures 3B and 3C) compared to the animal that did not receive treatment (photograph not shown) and the one that was administered the vehicle (Figure 3A) [63,66,67].

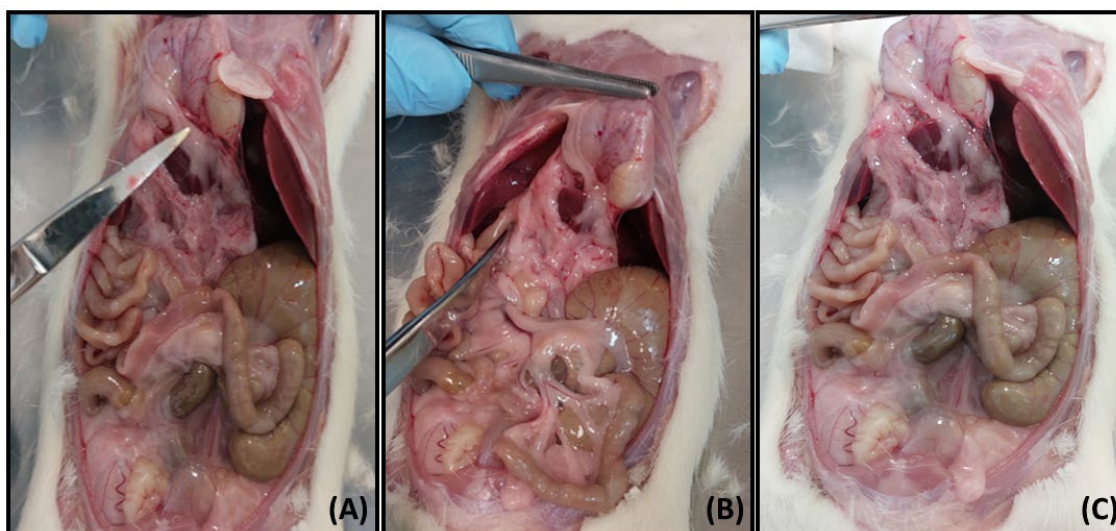


**Figure 3.** Necropsy performed on animals that were administered Vehicle (A), Compound **3b** (B) and Compound **4y** (C), both at a single dose of 1750 mg/kg.

Table 6 presents the values of the organ weights obtained after performing the corresponding necropsy following the acute administration of **3b** and **4y**. As can be seen, there was no significant difference in the weight of any of the organs extracted from the animals treated with both compounds compared to the organs of the animal that was administered with the vehicle. This suggests that **3b** and **4y** do not produce inflammation or other evident metabolic alterations that could have generated a significant increase or decrease in the weight of the organs.

**Table 6.** Weight of organs obtained from the necropsy performed 15 days after administration of compounds **3b** and **4y**.

Compound	Organ weight (g)				
	Spleen	Stomach	Liver	Intestine	Kidney
Vehículo	0.90	3.41	14.08	26.23	2.85
<b>3b</b> *	0.82 ± 0.05	2.93 ± 0.49	13.71 ± 2.11	25.04 ± 1.04	2.50 ± 0.04
<b>4y</b> *	0.84 ± 0.04	2.37 ± 0.40	14.71 ± 2.11	24.04 ± 0.94	2.95 ± 0.05

\* Compounds **3b** and **4y** were administered at a single dose of 1750 mg/kg.

### 2.2.2. Acute and Subchronic Effect of Compounds **3b** and **4y** in the Rat Model with T2D

Current protocols for the treatment of T2D are initially based on indicating to patients a non-pharmacological treatment consisting of a balanced diet and weight control; however, many of them also require a treatment based on the use of oral hypoglycemic agents to increase insulin sensitivity in adipose tissue, skeletal muscle and liver. Unfortunately, most drugs used to treat T2D have adverse effects. Therefore, the design or discovery of new agents with high antihyperglycemic activity, lipid profile control and fewer adverse effects becomes of great importance [63,68]. In order to establish the mechanisms of action of these compounds, various *in vivo* and *in vitro* models have been used, which in turn serve as a reference for the evaluation of new chemical entities with possible

antidiabetic activity. One of the rat models of T2D can be induced by administration of a single, low dose (35-60 mg/kg) of streptozotocin (STZ), which has been shown to produce hyperglycemia in rats as a result of its selective cytotoxicity on pancreatic beta cells and minimal toxicity to other organs compared to alloxan [63,67-72]. STZ increases the activity of xanthine oxidase and poly (ADP-ribose) polymerase (PARP), which consequently causes apoptotic and necrotic death of pancreatic beta cells. STZ is a nitric oxide (NO) donor and NO has been shown to induce pancreatic islet cell destruction and mediate restriction of mitochondrial ATP generation [72]. Following administration of animals with a single dose of STZ (45 mg/kg), a significant increase in blood glucose concentration was observed which ranged from 250 to 350 mg/dL. In addition, one group of animals received a single dose of 5 mg/kg of the drug glibenclamide (GBC) and blood glucose levels were monitored at 0.5, 1, 2, 3 and 4 h (Figure 1S). GBC produced a decrease in glucose values, suggesting that functional pancreatic beta cells are still present in the animals [73]. In this regard, GBC is known to be an oral hypoglycemic agent of the secretagogue type whose mechanism of action involves the blockade of ATP-dependent potassium channels, causing a depolarization of the plasma membrane and calcium gradient signaling, which induces increased insulin release [69].

#### 2.3.2.1. Food and Water Consumption and Body Weight

Figure 4A-4C shows the food and water consumption, as well as the body weight of the animals with T2D that were administered with compounds **3b** and **4y** in an equimolar ratio to PGZ (15 mg/kg) for 4 weeks. As can be seen in Figure 4A, in the T2D + **3b** and T2D + **4y** groups, food consumption remained constant from the beginning of treatment (week 1) to the end of it (week 4). In the T2D and T2D + PGZ groups, food consumption was significantly higher in week 4 compared to the beginning of treatment (week 1). In Figure 4B it can be observed that water consumption was significantly lower in the T2D + **3b** group in week 4 compared to week 1, while in the T2D + **4y** and T2D + PGZ groups water consumption remained constant and, in the T2D group, there was a significant decrease in week 4 compared to the start of treatment (week 1). In Figure 4C, it can be observed that in the T2D + **3b** group, the body weight of the animals increased significantly in week 4 with respect to week 1, and in the T2D + **4y** group there was also an increase, although this was not significant with respect to time. In the Control and T2D + PGZ groups, the weight also increased significantly in week 4 with respect to the beginning of the treatment (week 1), while in the T2D group the weight remained constant. In this regard, it is well known that PGZ is capable of producing the differentiation of adipose tissue in animals with T2D through the activation of PPAR gamma, which was demonstrated in this study [63-Álvarez; 67-Alemán]. It is noteworthy that, although the weight of T2D animals administered compounds **3b** and **4y** increased during the treatment period (week 1-4), it was lower compared to that of the group administered PGZ, suggesting that both compounds do not induce adipogenesis compared to this drug.

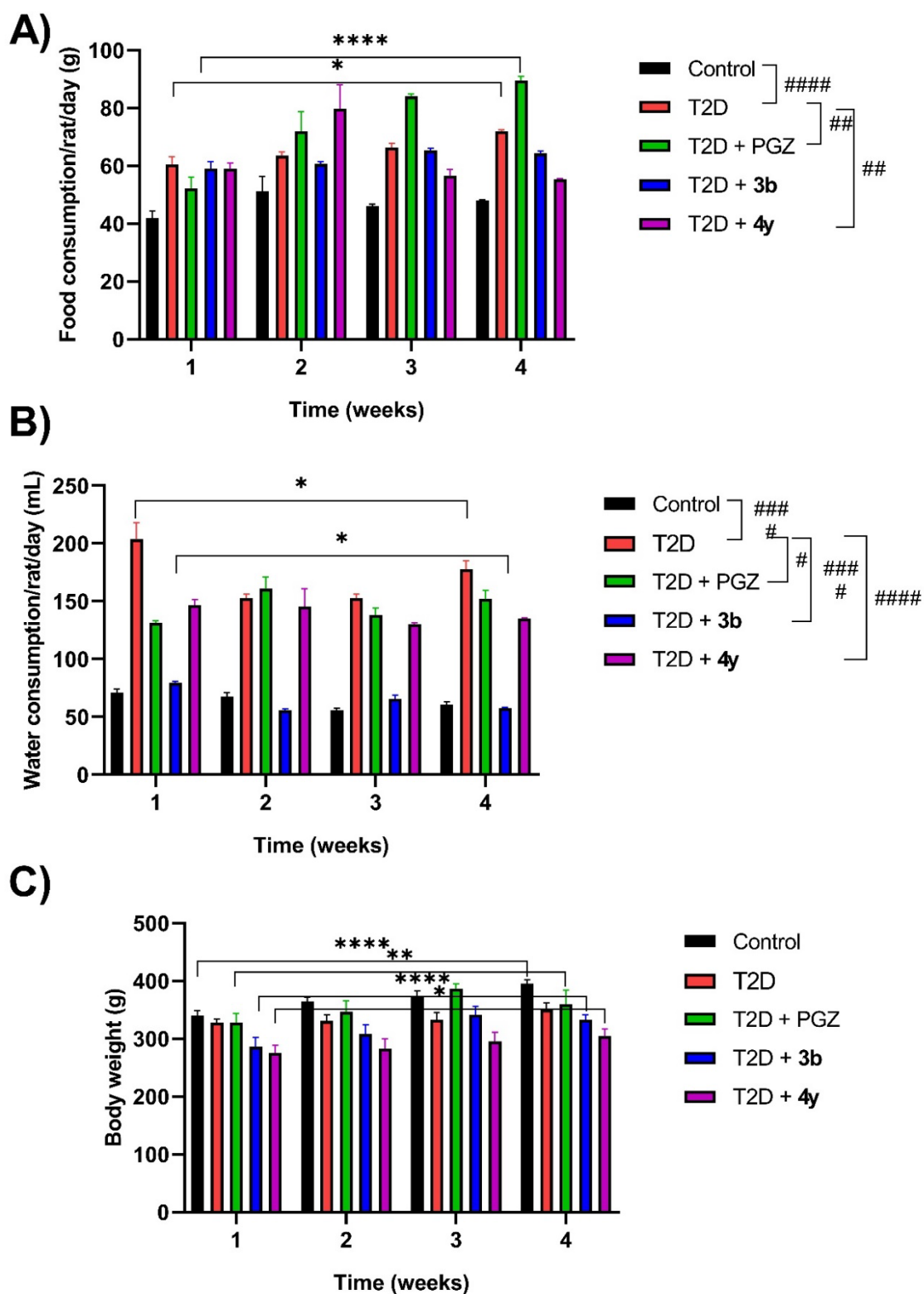


**Figure 4.** Food consumption (A), water consumption (B) and body weight (C) of T2D animals administered compounds **3b** and **4y** in equimolar ratio to PGZ (15 mg/kg) for 4 weeks. Data are expressed as mean  $\pm$  SEM and were analyzed by two-way ANOVA with Tukey's post-hoc test;  $n = 6$ . The graphs represent the most significant differences of each treatment group with respect to time (\*week 1 vs week 4) and between groups at the end of treatment (#week 4). Food consumption: \* $p < 0.1$ : T2D; \*\*\*\* $p < 0.0001$ : T2D + PGZ; # $p < 0.01$ : T2D vs T2D + PGZ, T2D vs T2D + **4y**; ### $p < 0.0001$ : Control vs T2D. Water consumption: \* $p < 0.1$ : T2D, T2D + **3b**; # $p < 0.1$ : T2D vs T2D + PGZ; ### $p <$

0.0001: Control vs T2D, T2D vs T2D + **3b**, T2D vs T2D + **4y**. Body weight: \* $p < 0.1$ : T2D + **4y**; \*\* $p < 0.01$ : T2D + PGZ; \*\*\*\* $p < 0.0001$ : Control, T2D + **3b**.

On the other hand, despite the fact that T2D animals consumed food and water constantly and even in greater quantities (in the case of water) than the rest of the experimental groups (T2D + PGZ, T2D + **3b** and T2D + **4y**), their body weight did not change significantly (Figure 4A-4C). These results are similar to the symptoms of T2D patients, which include weight loss despite polyphagia (increased food consumption), polydipsia (increased water consumption) and polyuria (increased urinary volume generation) [63,67]. STZ-induced diabetes is also characterized by weight loss, the decrease of which is due to the degradation of structural proteins such as those that form part of skeletal muscle (cachexia), since it is known that these contribute to weight gain [74]. This was clearly demonstrated in this study, since although there was no significant decrease in the weight of animals with T2D, it was lower compared to that of animals in the Control group during the treatment period (week 1-4).

Following acute and subchronic administration of compounds **3b** and **4y** in equimolar ratio to PGZ (15 mg/kg), blood glucose concentration and HbA1c percentage were measured (Figure 5A-5C). Figure 5A shows that blood glucose levels in animals in the T2D + **3b** group decreased significantly from 1 h to 4 h and in those in the T2D + **4y** group from 2 h to 4 h, both cases with respect to the initial value (0 h). In animals in the T2D + PGZ group, blood glucose concentration decreased significantly from 0.5 h to 4 h with respect to the start (0 h). In addition, the T2D + **4y** and T2D + PGZ groups showed significant differences with the T2D group and the latter with the Control group. It is worth noting that in the T2D + **3b** and T2D + **4y** groups there was no decrease in blood glucose levels below that of the Control group, so these results suggest that, like PGZ, compounds **3b** and **4y** do not cause hypoglycemia in healthy subjects or in those with T2D below normal values [63]. Regarding the subchronic administration of **3b** and **4y**, Figure 5B shows that blood glucose concentration decreased significantly in both groups from week 1 until the end of treatment (week 4), as in the T2D + PGZ group. However, as can be seen in the graph, unlike the T2D + **3y** and T2D + **4y** groups, blood glucose values in the T2D + PGZ group did not reach normal levels (< 100 mg/dL) at week 4, which is consistent with what has been reported in previous studies [63,67,75]. HbA1c is a sensitive marker used to detect early diabetes in high-risk individuals [74]. Figure 5C shows that the percentage of HbA1c in the T2D + **3b**, T2D + **4y**, and T2D+PGZ groups decreased at week 4 from baseline (week 1). Furthermore, the percentage of HbA1c also decreased in the three aforementioned groups compared to the T2D group, but without reaching the values of the Control group at week 4 of treatment. In this regard, it has been shown that the percentage of HbA1c strongly correlates with fasting blood glucose concentration in patients with diabetes. Glycation of hemoglobin is irreversible during the 120 days of life of red blood cells in the body. The assessment of changes in blood glucose levels is cumulative over a period of 4 to 8 weeks [76]. The percentage of HbA1c is stable, does not vary during the day and does not depend on recent changes in diet. Hemoglobin has free access to glucose, which passively diffuses through the red blood cell membrane. However, the glycation mechanism increases due to glycemic stress caused by the metabolic disturbance produced by the diabetic state [76]. In the present study, a significant increase in HbA1c levels was observed in addition to hyperglycemia in rats with T2D compared to healthy control indicating their poor glycemic status, as previously reported [74,76]. However, this metabolic alteration decreased with the administration of compounds **3b** and **4y**, as well as with PGZ.

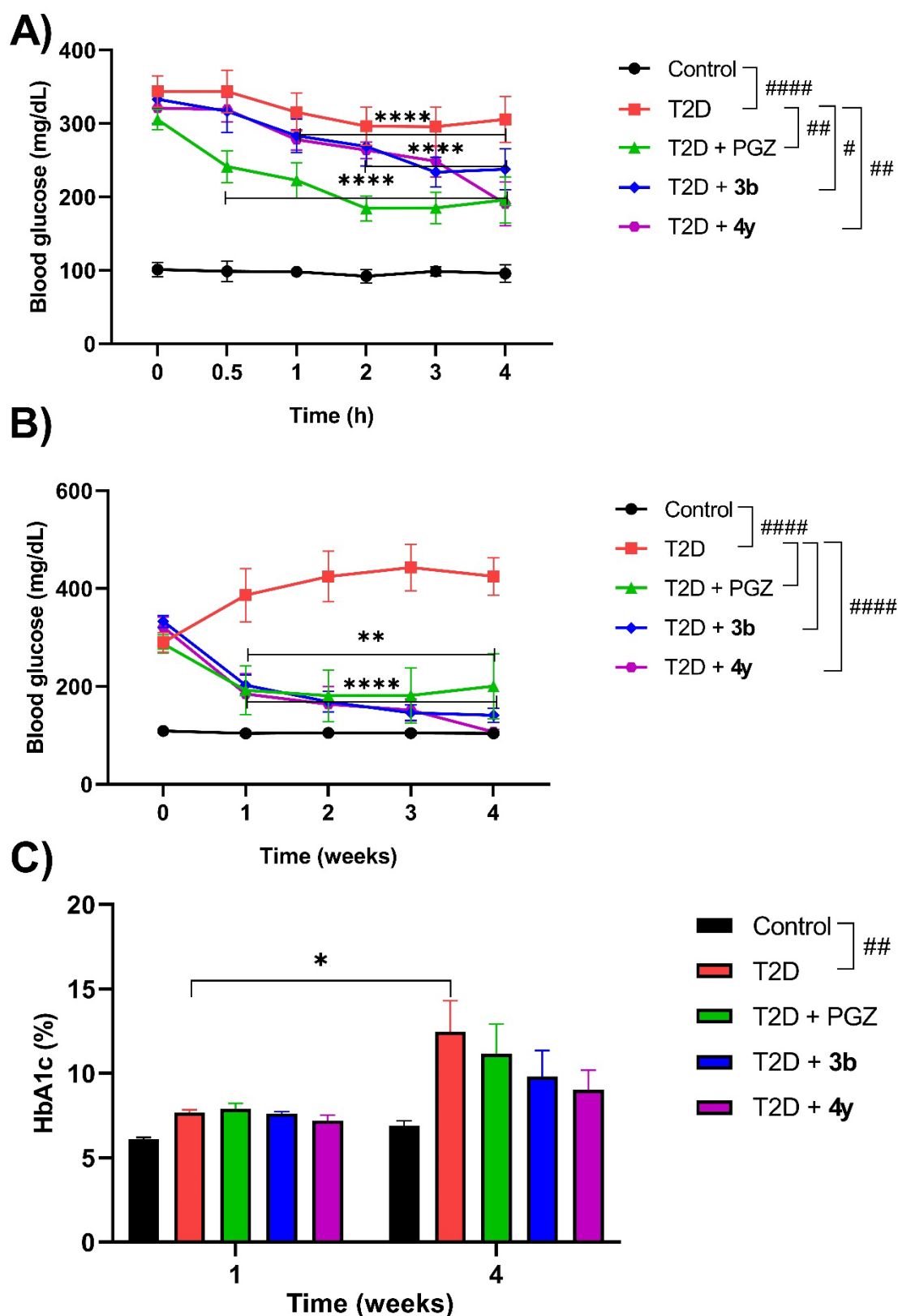


**Figure 5.** Blood glucose levels in T2D animals administered compounds **3b** and **4y** in equimolar ratio to PGZ (15 mg/kg) as a single dose in the acute trial (A), with repeated doses for 4 weeks in the subchronic trial (B), and percentage of HbA1c (C). Data are expressed as mean  $\pm$  SEM and were analyzed by two-way ANOVA with Tukey's post hoc test;  $n = 6$ . The graphs show the most significant differences between each treatment group over time (\*0 h vs 4 h; \*week 1 vs week 4) and between groups at the end of treatment (#4 h; #week 4). Blood glucose (ensayo agudo): \*\*\*\* $p < 0.0001$ ; T2D +

PGZ, T2D + **3b**, T2D + **4y**; #p < 0.1: T2D vs T2D + **3b**; ##p < 0.01: T2D vs T2D + PGZ; T2D vs T2D + **4y**; ###p < 0.0001: Control vs T2D. Blood glucose (ensayo subcrónico): \*\*p < 0.01: T2D + PGZ; \*\*\*\*p < 0.0001: T2D + **3b**, T2D + **4y**; ###p < 0.0001: Control vs T2D, T2D vs T2D + PGZ, T2D vs T2D + **3b**, T2D vs T2D + **4y**. HbA1c percentage: \*p < 0.1: T2D; ##p < 0.01: Control vs T2D.

Regarding the lipid profile, it can be observed in Table 7 that in animals with T2D administered with compounds **3b** and **4y**, the concentrations of triglycerides (TG), total cholesterol (T-Cho) and low-density lipoproteins (LDL-C) decreased with respect to the T2D group, while high-density lipoproteins (HDL-C) increased (week 4). It is worth mentioning that these results are comparable with those of the T2D + PGZ group, the effect of this drug on the lipid profile being well demonstrated in previous studies [63,67,74,75].

**Table 7.** Lipid profile of animals with T2D administered compounds 3b and 4y in equimolar ratio to PGZ (15 mg/kg) for 4 weeks.

Group	Parameter			
	TG (mg/dL)	T-Cho (mg/dL)	HDL-C (mg/dL)	LDL-C (mg/dL)
Control	107 ± 8	85 ± 3	10 ± 0	83 ± 3
T2D	128 ± 29	95 ± 11	12 ± 1	92 ± 10
T2D + PGZ	65 ± 14	79 ± 4	14 ± 2	76 ± 4
T2D + <b>3b</b>	91 ± 12	79 ± 3	13 ± 1	76 ± 2
T2D + <b>4y</b>	71 ± 15	74 ± 3	14 ± 2	71 ± 3

Abbreviations: T2D: type 2 diabetes; PGZ: pioglitazone; TG: triglycerides; T-Cho: total cholesterol; HDL-C: high-density lipoproteins; LDL-C: low-density lipoproteins. Data are expressed as mean ± SEM and were analyzed by one-way ANOVA with Tukey's post-hoc test; n = 6.

Oxidative stress may also play a central role in the pathogenesis of diabetic complications such as impaired glucose and lipid metabolism that promote hyperglycemia and dyslipidemia through overproduction of reactive oxygen species (ROS). These complications are associated with the development of atherosclerosis and cardiovascular diseases. Hyperglycemia is accompanied by elevated levels of TG, T-Cho, and LDL-C and decreased HDL-C levels in diabetic rats, in which the abnormally high serum lipid concentrations are mainly due to increased mobilization of free fatty acids from fat stores. Insulin activates the enzyme lipoprotein lipase (LPL) that hydrolyzes TG under normal conditions, however, it is not activated in the diabetic state due to insulin deficiency, resulting in hypertriglyceridemia. Circulating LDL-C is recaptured in the liver through specific receptors that clear the circulation. The increased serum LDL-C concentration in diabetic rats could be due to a defect in the LDL-C receptor, either through a failure in its production or function. ROS can stimulate the oxidation of LDL-C which can be taken up by scavenger receptors in macrophages leading to the formation of foam cells and atherosclerotic plaques. HDL-C is a cardioprotective lipid by reversing T-Cho transport, thus neutralizing the atherogenic effect of oxidized LDL-C, preventing coronary heart disease. The greater decrease in HDL-C could be due to the greater increase in LDL-C and VLDL-C since there is a reciprocal relationship between VLDL-C and HDL-C concentration. The decreased activity of the enzyme lecithin cholesterol acyltransferase (LCAT) could be responsible for the decreased activity of HDL-C [74,75]. In this study, animals with T2D administered compounds **3b** and **4y** showed an increase in HDL-C and a reduction in TG, T-Cho and LDL-C, so these results confirm that both compounds, like PGZ, can reduce the risk of cardiovascular diseases by restoring the unbalanced lipid profile.

In Table 8 it can be observed that the administration of compounds **3b** and **4y** to animals with T2D did not produce a significant change in the serum concentrations of the enzymes alanine aminotransferase (ALT/GPT), aspartate aminotransferase (AST/GOT) and gamma-glutamyl transferase (GGT) with respect to the Control group.

**Table 8.** Catalytic activity of liver enzymes in animals with T2D administered compounds **3b** and **4y** in equimolar ratio to PGZ (15 mg/kg) for 4 weeks.

Grupo	Parameter		
	ALT/GPT (U/L)	AST/GOT (U/L)	GGT (U/L)
Control	53 ± 7	263 ± 26	10 ± 0
T2D	57 ± 12	194 ± 19	11 ± 2
T2D + PGZ	54 ± 11	285 ± 11	12 ± 1
T2D + <b>3b</b>	31 ± 2	211 ± 14	10 ± 0
T2D + <b>4y</b>	49 ± 9	236 ± 28	10 ± 0

Abbreviations: T2D: type 2 diabetes; PGZ: pioglitazone; ALT/GPT: alanine aminotransferase; AST/GOT: aspartate aminotransferase; GGT: gamma-glutamyl transferase. Data are expressed as mean ± SEM and were analyzed by one-way ANOVA with Tukey's post hoc test; n = 6.

These results are similar to those observed in the T2D + PGZ group, as well as with previous studies in which it has been shown that this drug does not produce an increase in the catalytic activity of liver enzymes in both rats and humans with T2D [63,75]. Furthermore, since these results correlate with those obtained in the *in silico* study, as well as with the macroscopic analysis performed after subchronic treatment with **3b** and **4y**, in which it was shown that both compounds do not cause tissue damage, particularly at the hepatic level (data not shown), it is suggested that they are safe and do not produce harmful effects on the liver. On the contrary, in animals administered with PGZ there was an increase in adipose tissue which is well known to be one of the adverse effects of TZDs [63,75].

In summary, compounds **3b** and **4y** administered to animals with T2D favor the decrease of blood glucose concentration and improve dyslipidemia, which could be explained based on a mechanism of action similar to that of PGZ that improves insulin sensitivity throughout the body, instead of stimulating its secretion from pancreatic beta cells. In addition, the attenuating effect on hyperlipidemia (although not significant) could result either from the inhibition of TG synthesis in the liver or from the increase in its clearance in the periphery by stimulating the LPL enzyme and/or the inhibition of intestinal absorption of dietary T-Chol.

### 3. Materials and Methods

#### 3.1. Chemicals

All chemical reagents and solvents were of standard analytical grade and used without further purification (Sigma Aldrich; Toluca, State of Mexico, Mexico). For the quantification of metabolic (glucose, HbA1c, TG, T-Chol, HDL-C and LDL-C) and hepatic parameters (ALT/GPT, AST/GOT and GGT) solid-phase test strips with a coded chip (SPOTCHEM KENSHIN-2, Cat.: 77188, Arkray; Kyoto, Japan) were used. The synthesis and structural identification of compounds **3b** and **4y** was carried out based on previously reported data [44,46,48], with slight modifications that are described in the Supplementary Materials.

#### 3.2. *In Silico* Studies

##### 3.2.1. ADMET Properties Prediction

The 49-compound library was generated from two different series containing the 2-aminobenzothiazole nucleus linked to isothioureas (**3a-w**) or guanidines (**4a-z**). The chemical structures were drawn and the Simplified Molecular Input Line Entry System (SMILES) code of each compound was obtained from the Molinspiration Cheminformatics online server [77]. The physicochemical properties obtained from the latter are molecular weight (MW), octanol-water partition coefficient (cLogP), number of hydrogen bond acceptors (nON) and donors (nOHNH), number of rotatable bonds (nrotb) and topological polar surface area (TPSA), among others. On the other hand, with the DataWarrior [78], in addition to obtaining some of the aforementioned

properties (PM, cLogP, ASPT, etc.), the prediction of the toxicity risk of the compounds with respect to mutagenicity (M), tumorigenicity (T), irritant effects (IE) and reproductive effects (RE) was made. These theoretical characteristics were considered to assign an overall drug-likeness score (ODLS) to the evaluated compounds in order to select the best ones, that is, those that comply with Lipinski's rule of five [50,51] and the recommendations of Veber et al. [52]. Subsequently, the prediction of aqueous solubility (logS), pharmacokinetic properties (absorption, metabolism and toxicity) and medicinal chemistry of the compounds selected from the previous virtual screening was obtained using the SMILES code on the online servers Tox-Prediction [79] and SwissADME [80].

### 3.2.2. Analysis of the Binding Mode and Ligand-Protein Interactions by Molecular Docking

In order to establish whether one of the molecular targets of interest in diabetes that was more closely related to the proposed ligands is PPAR gamma, a reverse molecular docking study was first performed using the online server DIA-DB (<http://bio-hpc.eu/software/dia-db/>) and the reference drug PGZ, considering the association of its mechanism of action with that of other previously reported benzothiazole derivatives [23,39–43]. Therefore, a conventional (direct) molecular docking study was performed. Two-dimensional (2D) structures of the proposed ligands were drawn and pre-optimized using ChemSketch ([https://www.acdlabs.com/products/draw\\_nom/draw/chemsketch/](https://www.acdlabs.com/products/draw_nom/draw/chemsketch/)) and then saved in \*.mol format. Subsequently, the integrity of the ligands was verified, the structures were energetically minimized using a MMFF molecular mechanics method in Spartan Student Edition (Version '08) (<https://www.wavefun.com/>) and the generated file was saved in \*.spartan format. All torsions were allowed for rotation during molecular docking and the generated \*.mol file was converted to \*.pdb format with Spartan Student Edition (Version '08) (<https://www.wavefun.com/>). The crystal of the protein of interest was chosen from the RCSB PDB database (<https://www.rcsb.org/>), from which the third-dimensional (3D) structure and PDB conformers of it were obtained. Specifically, the PPAR gamma crystal chosen was the one with identification (ID) code 2PRG (<https://www.rcsb.org/structure/2PRG>) [81].

Subsequently, to carry out the molecular docking studies between the ligands and the protein, the Molegro Virtual Docker program (<http://molexus.io/molegro-virtual-docker/>) was used, and the study was directed. First, the method was validated, with the selection criterion being a root mean square deviation (RMSD) value  $< 2 \text{ \AA}$ . For the PPAR gamma protein crystal (2PRG), the coordinates were  $X = 49.31$ ,  $Y = -37.06$ ,  $Z = 19.13$ , with a radius of  $10 \text{ \AA}$ , using 3 search algorithms (MoldDock Optimaizer, MoldDock SE and Iterated simplex) and 4 scoring functions (MoldDock Score, MoldDock Score GRID, PLANTS Score and PLANTS Score GRID). 10 runs were performed with selected method (MoldDock Optimaizer search algorithm and PLANT Score scoring function), 1,500 maximum iterations in a population size of 50. Once the method was validated with the co-crystallized PPAR gamma ligand [81], the reference ligand PGZ was subjected to the previously established conditions to determine its binding mode and affinity for said protein. In addition, the dominant microspecies at physiological pH (7.4) was searched for using the MarvinSketch program and the necessary modifications were made before starting the molecular docking with each of the ligands to be evaluated. At the end of this procedure, the generated files of each ligand were exported to a format with \*.pdb extension for the subsequent analysis of the ligand-protein interactions by using the Drug Discovery and PyMOL programs that allow the visualization of the interactions in 2D and 3D, respectively. In addition, the  $\Delta G$  value of each of the ligand-protein interactions was calculated using the PRODIGY (PROtein binDing enerGY prediction) online server [82].

### 3.3. *In Vivo* Studies

#### 3.3.1. Animals

Male Wistar rats weighing  $200 \pm 20 \text{ g}$  were acquired from the Centro de Investigación y de Estudios Avanzados (CINVESTAV) del Instituto Politécnico Nacional (IPN) Unidad Zacatenco. They were housed in polypropylene cages under controlled temperature conditions ( $20\text{--}25 \text{ }^\circ\text{C}$ ) and

light/dark cycles of 12 x 12 h, with food (standard) and water ad libitum. Before performing the experiments, the animals were adapted to their new habitat during a one-week acclimatization period. All animals were handled and euthanized in accordance with humane endpoint considerations [83,84].

The study was conducted in accordance with the guidelines of the Declaration of Helsinki and based on the ARRIVE Essential 10 guidelines for the protocol for the use of laboratory animals [85]. The protocol was approved by the Institutional Research Committee on the Care and Use of Laboratory Animals (ESM-CICUAL-02/20-03-2013) of the Escuela Superior de Medicina (ESM) of the Instituto Politécnico Nacional (IPN), Mexico City, Mexico. It complies with the Mexican norm for this matter (NOM-062-ZOO-1999, Technical Specifications for the Production, Care, and Use of Laboratory Animals, SAGARPA), as well as the Guide for the Care and Use of Laboratory Animals of the National Research Council and National Institutes of Health (NIH Publications No. 8023, revised 1978).

### 3.3.2. Experimental Design

Animals were randomly assigned for all experiments. Specifically, group organization for the evaluation of compounds **3b** and **4y** in the T2D model was carried out as described in Table 9.

**Table 9.** Distribution of animals for the evaluation of the pharmacological effect of compounds **3b** and **4y**.

EXPERIMENTAL GROUPS			
HEALTHY		WITH T2D	
Name	Treatment	Name	Treatment
Healthy without treatment (n = 6)		T2D without treatment (n = 6)	STZ, 45 mg/kg *Note 1
Healthy + Vehículo (n = 6)	Vehicle, 1 mL *Note 2	T2D + Vehicle (n = 6)	STZ, 45 mg/kg + Vehicle, 1 mL
Healthy + PGZ (n = 6)	PGZ, 15 mg/kg	T2D + PGZ (n = 6)	STZ, 45 mg/kg + PGZ, 15 mg/kg
Healthy + <b>3b</b> or <b>4y</b> (n = 6)	Compound <b>3b</b> or <b>4y</b> *Note 3	T2D + <b>3b</b> or <b>4y</b> (n = 6)	STZ, 45 mg/kg + Compound <b>3b</b> or <b>4y</b>

Abbreviations: T2D: type 2 diabetes; STZ: streptozotocin; PGZ: pioglitazone; **3b**: N'-(1,3-benzothiazol-2-yl)-N-methyl(methylsulfanyl)metanimidamide; **4y**: N''-(1,3-benzothiazol-2-yl)-N,N'-di-tert-butylguanidine. \*Note 1: STZ dissolved in 0.1 M citrate buffer, pH = 4.5. \*Note 2: PGZ, **3b** or **4y** dissolved in water + Tween 80 + mineral oil (45:10:45). \*Note 3: **3b** or **4y** administered in equimolar ratio to PGZ (15 mg/kg).

### 3.3.3. Acute Oral Toxicity (AOT) Evaluation

The LD50 value of compounds **3b** and **4y** was estimated using the Up-and-Down method of OECD Guideline 425 [65]. According to the latter, a male Wistar rat (200 ± 20 g) was administered a dose of 175 mg/kg and was observed continuously for 48 h. As the animal survived, another animal received an increasing dose of 550 mg/kg (progression factor 3.2). As there were no toxic effects in the second rat, a third animal received an increasing dose of 1750 mg/kg and as it did not die either, two others were administered the same dose. All animals were kept under observation for 14 days and 24 h later they were taken to the humane endpoint for macroscopic examination of organs and tissues. Finally, the LD50 value of the compounds was estimated to determine their degree of toxicity and classify them based on the GHS [56].

### 3.3.4. Acute and Subchronic Assessment in the T2D Model

One week after the acclimatization period (week 0), animals were fasted for 12 h and then administered a single dose of 45 mg/kg STZ dissolved in 0.1 M citrate buffer pH 4.5 intraperitoneally (i.p.). Whole blood glucose levels were measured with a glucometer (FreeStyle, Optium Neo) and corresponding strips (FreeStyle, Optium) every third day for 1 week, with samples obtained by venipuncture of the rat's tail. Animals that maintained a blood glucose level between 250-350 mg/dL were considered for the study [8,63,67–72]. In order to corroborate that the generated model was closer to the pathophysiological characteristics of T2D, the animals with hyperglycemia were administered the twelfth day after the administration of STZ (week 2) with the drug GBC (secretagogue) at a dose of 5 mg/kg and the changes in blood glucose levels were measured at 0.5, 1, 2, 3, and 4 h, waiting for them to decrease [73].

In the second week after STZ administration and induction of the T2D model, animals were administered orally (p.o.) with compounds **3b** or **4y** at an equimolar dose relative to the positive control (PGZ, 15 mg/kg; Aurax®, Farmacia San Pablo, CDMX, Mexico) [75,86]. For the acute evaluation, blood glucose concentration was first measured (time 0) in the animals; subsequently, they received a single dose of PGZ and then blood glucose concentration was measured again at 0.5, 1, 2, 3, and 4 h, in order to observe the effect of the treatment administered in the animals. In the case of subchronic evaluation, compounds **3b** or **4y** were administered daily at the previously mentioned dose (equimolar ratio with PGZ, 15 mg/kg) and blood glucose levels were monitored every 7 days until the end of treatment in the fourth week after its initiation. In addition, quantification of HbA1c, TG, T-Cho, HDL-C and LDL-C, as well as the catalytic activity of the enzymes ALT/GPT, AST/GOT and GGT were performed at the end of treatment in order to demonstrate its effectiveness. For this purpose, blood samples were obtained by venipuncture of the rat's tail and, only in the case of HbA1c, it was immediately measured from a whole blood sample using a portable analyzer (BioHermes, GluCoA1c) and test kit (BioHermes, GluCoA1c Glycohemoglobin Test Kit), while for the determination of the other parameters, the blood samples were kept at room temperature for 30 min and then centrifuged at 4000 RPM for 15 min at 4 °C. Finally, the serum was stored at –8 °C until it was measured in an automated dry chemistry analyzer (Arkray, SPOTCHEM EZ) and the use of strips for the quantification of the aforementioned parameters (SPOTCHEM II KENSHIN-2 (GPT, GOT, GGT, TG, T-Cho, HDL-C), in a maximum period of 2 days [75].

### 3.3.5. Record of Food and Water Consumption and Body Weight

Food and water consumption were monitored every third day. The animals' body weight was also recorded from the day of their arrival at their new accommodation and then every 7 days throughout the study [8,63].

## 3.4. Ex Vivo Studies

### 3.4.1. Sample Collection and Processing

At the end of the treatments (week 4), the animals were fasted for 12 h and the following day the last blood samples were obtained (following the previously described procedure) before being taken to the humane endpoint. Once the animals were sacrificed, a macroscopic examination of the organs and tissues was performed to rule out signs of toxicity induced by the subchronic administration of compounds **3b** or **4y** [75].

## 3.5. Statistic Analysis

Data obtained in the in vivo studies are expressed as mean  $\pm$  standard error of the mean (SEM) with  $n = 6$ . For all parameters, comparisons between groups were carried out using a two-way analysis of variance (ANOVA) followed by Tukey's multiple comparisons test. All statistical tests were performed and graphed using GraphPad software, version 8.2.1, where a  $p$  value  $< 0.05$  was considered to indicate whether there was a significant difference in each group with respect to time and between each treatment.

#### 4. Conclusions

Compounds **3a**, **3b**, **4a**, **4b**, **4c**, **4r**, **4s**, **4x**, and **4y** selected from the in silico study could be useful for the treatment of T2D and its micro and macrovascular complications, based on their ADMET properties, as well as the  $\Delta G$  values obtained with the PPAR gamma protein. In this study, compounds **3b** and **4y** were evaluated in the T2D rat model, which have an antihyperglycemic and hypolipidemic effect, in addition to not causing liver damage, being compared with the reference drug PGZ. Therefore, it is suggested that the mechanism of action of both compounds could be associated with PPAR gamma agonism, although it is not ruled out that **3b** and **4y** may also act on other molecular targets, thus preventing micro and macrovascular complications of T2D. However, further preclinical trials are needed to clearly demonstrate the antidiabetic effect of both compounds before they can be evaluated in the clinical phase.

**Supplementary Materials:** The following supporting information can be downloaded at the website of this paper posted on Preprints.org.

**Author Contributions:** Conceptualization, J.A.A.S., M.V., and J.E.M.W.; Data curation, B.M.J. and D.P.G.; Formal analysis, J.A.A.S., M.V., and J.E.M.W.; Funding acquisition, J.E.M.W. and A.C.; Investigation, J.A.A.S., M.V., B.M.J., and J.E.M.W.; Methodology, J.A.A.S., M.V., A.C., B.M.J., D.P.G., and J.E.M.W.; Project administration, J.E.M.W.; Resources, A.C., J.E.M.W.; Supervision, J.A.A.S., M.V., A.C., I.M.O.C., F.T.C., and J.E.M.W. Software, J.A.A.S. and M.V.; Validation, J.A.A.S. and B.M.J.; Visualization, J.A.A.S. and M.V.; Writing—original draft, J.E.M.W.; Writing—review & editing, J.A.A.S., M.V., A.C., B.M.J., D.P.G., I.M.O.C., and F.T.C. All authors have read and agreed to the published version of the manuscript.

**Funding:** This research was funded by the Secretaría de Investigación y Posgrado of the Instituto Politécnico Nacional (grant numbers: SIP20240101; SIPMULTI2297).

**Institutional Review Board Statement:** The study was conducted in accordance with the guidelines of the Declaration of Helsinki and based on the ARRIVE Essential 10 guidelines for the protocol for the use of laboratory animals (<https://arriveguidelines.org/arrive-guidelines>). The protocol was approved by the Institutional Research Committee on the Care and Use of Laboratory Animals (ESM-CICUAL-02/20-03-2013) of the Escuela Superior de Medicina (ESM) of the Instituto Politécnico Nacional (IPN), Mexico City, Mexico. It complies with the Mexican norm for this matter (NOM-062-ZOO-1999, Technical Specifications for the Production, Care, and Use of Laboratory Animals, SAGARPA), as well as the Guide for the Care and Use of Laboratory Animals of the National Research Council and National Institutes of Health (NIH Publications No. 8023, revised 1978).

**Informed Consent Statement:** Not applicable.

**Data Availability Statement:** All the relevant data found in the study are available in the article. The data supporting the study are in Supplementary Materials section.

**Acknowledgments:** The authors would like to thank the Secretaría de Investigación y Posgrado of the Instituto Politécnico Nacional (grant numbers: SIP20240101; SIPMULTI2297) for supporting this research. B.M.J. thanks Consejo Nacional de Humanidades, Ciencias y Tecnologías (CONAHCYT) for her master scholarship (CVU: 754848).

**Conflicts of Interest:** The authors declare no conflict of interest. The funder had no role in the design of the study, in the collection, analyses, or interpretation of data, in the writing of the manuscript, or in the decision to publish the results.

#### References

1. Magliano, D.J.; Boyko, E.J.; Balkau, B.; Barengo, N.; Barr, E.; Basit, A.; Bhata, D.; Bommer, C.; Booth, G.; Cariou, B.; et al. International Diabetes Federation IDF Diabetes Atlas, 10th ed.; Berkeley Communications: Reading, UK, 2021; Volume 102, ISBN 9782930229980.
2. Al-Muzafar, H.M.; Alshehri, F.S.; Amin, K.A. The role of pioglitazone in antioxidant, anti-inflammatory, and insulin sensitivity in a high fat-carbohydrate diet-induced rat model of insulin resistance. *Braz. J. Med. Biol. Res.* **2021**, *54*, e10782.
3. Ashraf, S.A.; Elkhalfifa, A.E.O.; Mehmood, K.; Adnan, M.; Khan, M.A.; Eltoum, N.E.; Krishnan, A.; Baig, M.S. Multi-targeted molecular docking, pharmacokinetics, and drug-likeness evaluation of okra-derived

- ligand abscisic acid targeting signaling proteins involved in the development of diabetes. *Molecules* **2021**, *26*, 5957.
4. Dowarah, J.; Singh, V.P. Anti-diabetic drugs recent approaches and advancements. *Bioorg. Med. Chem.* **2020**, *28*, 115263.
  5. Harding, J.L.; Pavkov, M.E.; Magliano, D.J.; Shaw, J.E.; Gregg, E.W. Global trends in diabetes complications: A review of current evidence. *Diabetologia* **2019**, *62*, 3–16.
  6. Kousaxidis, A.; Petrou, A.; Lavrentak, i V.; Fesatidou, M.; Nicolaou, I.; Geronikaki, A. Aldose reductase and protein tyrosine phosphatase 1B inhibitors as a promising therapeutic approach for diabetes mellitus. *Eur. J. Med. Chem.* **2020**, *207*, 112742.
  7. Shiming, Z.; Mak, K.-K.; Balijepalli, M.K.; Chakravarthi, S.; Pichika, M.R. Swietenine potentiates the antihyperglycemic and antioxidant activity of metformin in streptozotocin induced diabetic rats. *Biomed. Pharmacother.* **2021**, *139*, 111576.
  8. Álvarez-Almazán, S.; Solís-Domínguez, L.C.; Duperou-Luna, P.; Fuerte-Gómez, T.; González-Andrade, M.; Aranda-Barradas, M.E.; Palacios-Espinosa, J.F.; Pérez-Villanueva, J., Matadamas-Martínez, F., Miranda-Castro, S.P.; et al. Anti-diabetic activity of glycyrrhetic acid derivatives FC-114 and FC-122: scale-up, in silico, in vitro, and in vivo studies. *Int. J. Mol. Sci.* **2023**, *24*, 12812.
  9. Tomic, D.; Shaw, J.E.; Magliano, D.J. The burden and risks of emerging complications of diabetes mellitus. *Nat. Rev. Endocrinol.* **2022**, *18*, 525–539.
  10. Sun, H.; Saeedi, P.; Karuranga, S.; Pinkepank, M.; Ogurtsova, K.; Duncan, B.B.; Stein, C.; Basit, A.; Chan, J.C.N.; Mbanya, J.C.; et al. IDF Diabetes Atlas: Global, regional and country-level diabetes prevalence estimates for 2021 and projections for 2045. *Diabetes Res. Clin. Pract.* **2022**, *183*, 109119.
  11. University of Oxford Our World in Data. Diabetes Prevalence. 2021. Available online: <https://ourworldindata.org/search?q=diabetes> (accessed on October 10, 2023).
  12. Bello-Chavolla, O.Y.; Antonio-Villa, N.E.; Fermín-Martínez, C.A.; Fernández-Chirino, L.; Vargas-Vázquez, A.; Ramírez-García, D.; Basile-Alvarez, M.R.; Hoyos-Lázaro, A.E.; Carrillo-Larco, R.M.; Wexler, D.J.; et al. Diabetes-related excess mortality in Mexico: a comparative analysis of national death registries between 2017–2019 and 2020. *Diabetes Care* **2022**, *45*, 2957–2966.
  13. U.S. Department of Health & Human Services What is diabetes? Available online: <https://www.cdc.gov/diabetes/basics/diabetes.html> (accessed on October 10, 2023).
  14. Almeida, C.; Monteiro, C.; Silvestre, S. Inhibitors of 11 $\beta$ -hydroxysteroid dehydrogenase type 1 as potential drugs for type 2 diabetes mellitus—a systematic review of clinical and in vivo preclinical studies. *Sci. Pharm.* **2021**, *89*, 5.
  15. Padhi, S.; Nayak, A.K.; Behera, A. Type II diabetes mellitus: A review on recent drug based therapeutics. *Biomed. Pharmacother.* **2020**, *131*, 110708.
  16. Simos, Y.V.; Spyrou, K.; Patila, M.; Karouta, N.; Stamatis, H.; Gournis, D.; Dounousi, E.; Peschos, D. Trends of nanotechnology in type 2 diabetes mellitus treatment. *Asian J. Pharm. Sci.* **2021**, *16*, 62–76.
  17. Yadav, R.K.; Kumar, R.; Singh, H.; Mazumdar, A.; Salahuddin, Chauhan, B.; Abdullah, M.M. Recent insights on synthetic methods and pharmacological potential in relation with structure of benzothiazoles. *Med. Chem.* **2023**, *19*, 325–360.
  18. Dahlén, A.D., Dashi, G., Maslov, I., Attwood, M.M., Jonsson, J., Trukhan, V., Schiöth, H.B. Trends in antidiabetic drug discovery: FDA approved drugs, new drugs in clinical trials and global sales. *Front. Pharmacol.* **2022**, *12*, 807548.
  19. Konkwo, C.; Perry, R.J. Imeglimin: Current development and future potential in type 2 diabetes. *Drugs* **2021**, *81*, 185–190.
  20. Artasensi, A.; Pedretti, A.; Vistoli, G.; Fumagalli, L. Type 2 diabetes mellitus: A review of multi-target drugs. *Molecules* **2020**, *25*, 1987.
  21. Seth, S. A comprehensive review on recent advances in synthesis & pharmacotherapeutic potential of benzothiazoles. *Antiinflamm. Antiallergy Agents Med. Chem.* **2015**, *14*, 98–112.
  22. Sumit, Kumar, A.; Mishra, A.K. Advancement in pharmacological activities of benzothiazole and its derivatives: An up to date review. *Mini Rev. Med. Chem.* **2021**, *21*, 314–335.
  23. Bhutani, R.; Pathak, D.P.; Kapoor, G.; Husain, A.; Iqbal, M.A. Novel hybrids of benzothiazole-1,3,4-oxadiazole-4-thiazolidinone: Synthesis, in silico ADME study, molecular docking and in vivo anti-diabetic assessment. *Bioorg. Chem.* **2019**, *83*, 6–19.
  24. Gupta, K.; Sirbaiya, A.K.; Kumar, V.; Rahman, M.A. Current perspective of synthesis of medicinally relevant benzothiazole based molecules: Potential for antimicrobial and anti-inflammatory activities. *Mini Rev. Med. Chem.* **2022**, *22*, 1895–1935.
  25. Haroun, M. Review on the developments of benzothiazole-containing antimicrobial agents. *Curr. Top Med. Chem.* **2022**, *22*, 2630–2659.
  26. Keri, R.S.; Patil, M.R.; Patil, S.A.; Budagumpi, S. A comprehensive review in current developments of benzothiazole-based molecules in medicinal chemistry. *Eur. J. Med. Chem.* **2015**, *89*, 207–251.
  27. Rouf, A.; Tanyeli, C. Bioactive thiazole and benzothiazole derivatives. *Eur. J. Med. Chem.* **2015**, *97*, 911–927.

28. Ciocci Pardo, A.; González Arbeláez, L.F.; Fantinelli, J.C.; Álvarez, B.V.; Mosca, S.M.; Swenson, E.R. Myocardial and mitochondrial effects of the anhydrase carbonic inhibitor ethoxzolamide in ischemia-reperfusion. *Physiol. Rep.* **2021**, *9*, e15093.
29. García-Fernández, M.J.; Tabary, N.; Martel, B.; Cazaux, F.; Oliva, A.; Taboada, P.; Concheiro, A.; Alvarez-Lorenzo, C. Poly-(cyclo)dextrins as ethoxzolamide carriers in ophthalmic solutions and in contact lenses. *Carbohydr. Polym.* **2013**, *98*, 1343–1352.
30. Modak, J.K.; Tikhomirova, A.; Gorrell, R.J.; Rahman, M.M.; Kotsanas, D.; Korman, T.M.; Garcia-Bustos, J.; Kwok, T.; Ferrero, R.L.; Supuran, C.T.; Roujeinikova, A. Anti-Helicobacter pylori activity of ethoxzolamide. *J. Enzyme Inhib. Med. Chem.* **2019**, *34*, 1660–1667.
31. Rahman, M.M.; Tikhomirova, A.; Modak, J.K.; Hutton, M.L.; Supuran, C.T.; Roujeinikova, A. Antibacterial activity of ethoxzolamide against Helicobacter pylori strains SS1 and 26695. *Gut Pathog.* **2020**, *12*, 20.
32. Chiò, A.; Mazzini, L.; Mora, G. Disease-modifying therapies in amyotrophic lateral sclerosis. *Neuropharmacology* **2020**, *167*, 107986.
33. Jaiswal, M.K. Riluzole and edaravone: A tale of two amyotrophic lateral sclerosis drugs. *Med. Res. Rev.* **2019**, *39*, 733–748.
34. Hatfield, S.M.; Hartley, L.W.; Schmidtke, J.R. The immunomodulatory action of frentizole, a novel immunosuppressive agent. *Immunopharmacology* **1982**, *5*, 169–179.
35. Aitken, L.; Benek, O.; McKelvie, B.E.; Hughes, R.E.; Hroch, L.; Schmidt, M.; Major, L.L.; Vinklarova, L.; Kuca, K.; Smith, T.K.; Musilek, K.; Gunn-Moore, F.J. Novel benzothiazole-based ureas as 17 $\beta$ -HSD10 inhibitors, a potential Alzheimer's disease treatment. *Molecules* **2019**, *24*, 2757.
36. Fišar, Z.; Musilek, K.; Benek, O.; Hroch, L.; Vinklářová, L.; Schmidt, M.; Hroudová, J.; Raboch, J. Effects of novel 17 $\beta$ -hydroxysteroid dehydrogenase type 10 inhibitors on mitochondrial respiration. *Toxicol. Lett.* **2021**, *339*, 12–19.
37. Hroch, L.; Guest, P.; Benek, O.; Soukup, O.; Janockova, J.; Dolezal, R.; Kuca, K.; Aitken, L.; Smith, T.K.; Gunn-Moore, F.; Zala, D.; Ramsay, R.R.; Musilek, K. Synthesis and evaluation of frentizole-based indolyl thiourea analogues as MAO/ABAD inhibitors for Alzheimer's disease treatment. *Bioorg. Med. Chem.* **2017**, *25*, 1143–1152.
38. Badawy, D.; El-Bassossy, H.M.; Fahmy, A.; Azhar, A. Aldose reductase inhibitors zopolrestat and ferulic acid alleviate hypertension associated with diabetes: effect on vascular reactivity. *Can. J. Physiol. Pharmacol.* **2013**, *91*, 101–107.
39. Bhutani, R.; Pathak, D.P.; Kapoor, G.; Husain, A.; Kant, R.; Iqbal, M.A. Synthesis, molecular modelling studies and ADME prediction of benzothiazole clubbed oxadiazole-Mannich bases, and evaluation of their anti-diabetic activity through in vivo model. *Bioorg. Chem.* **2018**, *77*, 6–15.
40. Gim, H.J.; Cheon, Y.J.; Ryu, J.H.; Jeon, R. Design and synthesis of benzoxazole containing indole analogs as peroxisome proliferator-activated receptor- $\gamma/\delta$  dual agonists. *Bioorg. Med. Chem. Lett.* **2011**, *21*, 3057–3061.
41. Haroun, M. Novel Hybrids of pyrazolidinedione and benzothiazole as TZD analogues. rationale design, synthesis and in vivo anti-diabetic evaluation. *Med. Chem.* **2019**, *15*, 624–633.
42. Haroun, M. In silico design, synthesis and evaluation of novel series of benzothiazole-based pyrazolidinediones as potent hypoglycemic agents. *Med. Chem.* **2020**, *16*, 812–825.
43. Kharbanda, C.; Alam, M.S.; Hamid, H.; Javed, K.; Bano, S.; Ali, Y.; Dhulap, A.; Alam, P.; Pasha, M.A. Novel piperine derivatives with antidiabetic effect as PPAR- $\gamma$  agonists. *Chem. Biol. Drug Des.* **2016**, *88*, 354–362.
44. Cruz, A.; Padilla-Martínez, I.I.; García-Báez, E.V. A synthetic method to access symmetric and non-symmetric 2-(N,N'-disubstituted)guanidinebenzothiazoles. *Molecules* **2012**, *17*, 10178–10191.
45. Mendieta-Wejbe, J.E.; Rosales-Hernández, M.C.; Padilla-Martínez, I.I.; García-Báez, E.V.; Cruz, A. Design, synthesis and biological activities of (thio)urea benzothiazole derivatives. *Int. J. Mol. Sci.* **2023**, *24*, 9488.
46. Padilla-Martínez, I.I.; González-Encarnación, J.M.; García-Báez, E.V.; Cruz, A.; Ramos-Organillo, Á.A. Isothioureas, ureas, and their N-methyl amides from 2-aminobenzothiazole and chiral amino acids. *Molecules* **2019**, *24*, 3391.
47. Rosales-Hernández, M.C.; Mendieta-Wejbe, J.E.; Padilla-Martínez, I.I.; García-Báez, E.V.; Cruz, A. Synthesis and biological importance of 2-(thio)ureabenzothiazoles. *Molecules* **2022**, *27*, 6104.
48. Rosales-Hernández, M.C.; Mendieta-Wejbe, J.E.; Tamay-Cach, F.; Cruz, A. Synthetic procedures to access 2-guanidinobenzazoles of biological interest. *Curr. Org. Synth.* **2023**, *20*, 504–522.
49. Rosales-Hernández, M.C.; Cruz, A.; Mendieta-Wejbe, J.E.; Tamay-Cach, F. 2-Guanidinobenzazoles as building blocks to afford biologically active derivatives. *Curr. Org. Chem.* **2023**, *27*, 38–54.
50. Lipinski C.A. Rule of five in 2015 and beyond: Target and ligand structural limitations, ligand chemistry structure and drug discovery project decisions. *Adv. Drug Deliv. Rev.* **2016**, *101*, 34–41.
51. Lipinski, C.A.; Lombardo, F.; Dominy, B.W.; Feeney, P.J. Experimental and computational approaches to estimate solubility and permeability in drug discovery and development settings. *Adv. Drug Deliv. Rev.* **2001**, *46*, 3–26.
52. Veber, D.F.; Johnson, S.R.; Cheng, H.Y.; Smith, B.R.; Ward, K.W.; Kopple, K.D. Molecular properties that influence the oral bioavailability of drug candidates. *J. Med. Chem.* **2002**, *45*, 2615–2623.

53. Cornelissen, F.M.G., Market, G., Deutsch, G., Antonara, M., Faaij, N., Bartelink, I., Noske, D., Vandertop, W.P., Bender, A., Westerman, B.A. Explaining blood-brain barrier permeability of small molecules by integrated analysis of different transport mechanisms. *J. Med. Chem.* **2023**, *66*, 7253-7267.
54. Daina, A., Zoete, V. A BOILED-egg to predict gastrointestinal absorption and brain penetration of small molecules. *ChemMedChem.* **2016**, *11*, 1117-1121.
55. Prasanna, S.; Doerksen, R.J. Topological polar surface area: a useful descriptor in 2D-QSAR. *Curr. Med. Chem.* **2009**, *16*, 21-41.
56. United Nations Economic Commission for Europe. Sustainable Development Goals. About the GHS. Available online: <https://unece.org/about-ghs> (accessed on January 30, 2023).
57. Arana, M.R.; Altenberg, G.A. ATP-binding Cassette Exporters: Structure and Mechanism with a Focus on P-glycoprotein and MRP1. *Curr. Med. Chem.* **2019**, *26*, 1062-1078.
58. Beis K. Structural basis for the mechanism of ABC transporters. *Biochem. Soc. Trans.* **2015**, *43*, 889-893.
59. Di L. The role of drug metabolizing enzymes in clearance. *Expert Opin. Drug Metab. Toxicol.* **2014**, *10*, 379-393.
60. Chinnam, P.; Mohsin, M.; Shafee, L.M. Evaluation of acute toxicity of pioglitazone in mice. *Toxicol. Int.* **2012**, *19*, 250-254.
61. Muralikumar, S., Vetrivel, U., Narayanasamy, A., & N Das, U. Probing the intermolecular interactions of PPAR $\gamma$ -LBD with polyunsaturated fatty acids and their anti-inflammatory metabolites to infer most potential binding moieties. *Lipids Health Dis.* **2017**, *16*, 17.
62. Álvarez-Almazán, S.; Bello, M.; Tamay-Cach, F.; Martínez-Archundia, M.; Alemán-González-Duhart, D.; Correa-Basurto, J.; Mendieta-Wejebe, J.E. Study of new interactions of glitazone's stereoisomers and the endogenous ligand 15d-PGJ2 on six different PPAR gamma proteins. *Biochem. Pharmacol.* **2017**, *142*, 168-193.
63. Álvarez-Almazán, S.; Navarrete-Vázquez, G.; Padilla-Martínez, I.I.; Correa-Basurto, J.; Alemán-González-Duhart, D.; Tamay-Cach, F.; Mendieta-Wejebe, J.E. A new symmetrical thiazolidinedione derivative: in silico design, synthesis, and in vivo evaluation on a streptozotocin-induced rat model of diabetes. *Processes* **2021**, *9*, 1294.
64. Kroker, A.J.; Bruning, J.B. Review of the structural and dynamic mechanisms of PPAR $\gamma$  partial agonism. *PPAR Res.* **2015**, *2015*, 816856.
65. Organisation for Economic Co-operation and Development (OECD). OECD Guidelines for the Testing of Chemicals. Test Guideline No. 425. Acute Oral Toxicity: Up-and-Down-Procedure (UDP). Paris, France, 2008, p.p. 1-28. Available online: <https://www.oecd.org/env/test-no-425-acute-oral-toxicity-up-and-down-procedure-9789264071049-en.htm> (accessed on January 16, 2023).
66. Alemán-González-Duhart, D., Tamay-Cach, F., Correa-Basurto, J., Padilla-Martínez, I.I., Álvarez-Almazán, S., Mendieta-Wejebe, J.E. In silico design, chemical synthesis and toxicological evaluation of 1,3-thiazolidine-2,4-dione derivatives as PPAR $\gamma$  agonists. *Regul. Toxicol. Pharmacol.* **2017**, *86*, 25-32.
67. Alemán-González-Duhart, D., Álvarez-Almazán, S., Valdes, M., Tamay-Cach, F., & Mendieta-Wejebe, J. E. (2021). In vivo and ex vivo evaluation of 1,3-thiazolidine-2,4-dione derivatives as euglycemic agents. *PPAR Res.* **2021**, *2021*, 5100531.
68. Ahmed, Y.M., Abdelgawad, M.A., Shalaby, K., Ghoneim, M.M., AboulMagd, A.M., Abdelwahab, N.S., Hassan, H.M., Othman, A.M. Pioglitazone synthetic analogue ameliorates streptozotocin-induced diabetes mellitus through modulation of ACE 2/angiotensin 1-7 via PI3K/AKT/mTOR signaling pathway. *Pharmaceuticals* **2022**, *15*, 341.
69. Frederico, M.J.S., Castro, A.J.G., Menegaz, D., Murat, C.B., Mendes, C.P., Mascarello, A., Nunes, R.J., Silva, F.R.M.B. Mechanism of action of novel glibenclamide derivatives on potassium and calcium channels for insulin secretion. *Curr. Drug Targets* **2017**, *18*, 641-650.
70. Furman, B.L. Streptozotocin-induced diabetic models in mice and rats. *Curr. Protoc.* **2021**, *1*, e78.
71. Ghasemi, A., Jeddi, S. Streptozotocin as a tool for induction of rat models of diabetes: a practical guide. *EXCLI J.* **2023**, *22*, 274-294.
72. Kaur, R., Sodhi, R.K., Aggarwal, N., Kaur, J., Jain, U.K. Renoprotective effect of lansoprazole in streptozotocin-induced diabetic nephropathy in Wistar rats. *Naunyn Schmiedebergs Arch. Pharmacol.* **2016**, *389*, 73-85.
73. Valdés, M., Calzada, F., Mendieta-Wejebe, J.E., Merlín-Lucas, V., Velázquez, C., Barbosa, E. Antihyperglycemic effects of *Annona diversifolia* Safford and its acyclic terpenoids:  $\alpha$ -glucosidase and selective SGLT1 inhibitors. *Molecules* **2020**, *25*, 3361.
74. Madhuri, K., Naik, P.R. Modulatory effect of garcinol in streptozotocin-induced diabetic Wistar rats. *Arch. Physiol. Biochem.* **2017**, *123*, 322-329.
75. Abo-elmatty, D.M., Essawy, S.S., Badr, J.M., Sterner, O. Antioxidant and anti-inflammatory effects of *Urtica pilulifera* extracts in type 2 diabetic rats. *J. Ethnopharmacol.* **2013**, *145*, 269-277.

76. Lasram, M.M., Bouzid, K., Douib, I.B., Annabi, A., El Elj, N., El Fazaa, S., Abdelmoula, J., Gharbi, N. Lipid metabolism disturbances contribute to insulin resistance and decrease insulin sensitivity by malathion exposure in Wistar rat. *Drug Chem. Toxicol.* **2015**, *38*, 227–234.
77. Molinspiration Cheminformatics. Available online: <https://www.molinspiration.com> (accessed on September 21, 2022).
78. Openmolecules.org. DataWarrior. Available online: <https://openmolecules.org/datawarrior/> (accessed on September 25, 2022).
79. ProTox 3.0. Prediction of Toxicity of Chemicals. Tox-Prediction. Available on: [https://tox-new.charite.de/prottox\\_II/](https://tox-new.charite.de/prottox_II/) (accessed on October 5, 2022).
80. SwissADME. SwissDrugDesign. Available on: <http://www.swissadme.ch/> (accessed on October 12, 2022).
81. Nolte, R.T.; Wisely, G.B.; Westin, S.; Cobb, J.E.; Lambert, M.H.; Kurokawa, R.; Rosenfeld, M.G.; Willson, T.M.; Glass, C.K.; Milburn, M.V. Ligand binding and co-activator assembly of the peroxisome proliferator-activated receptor-gamma. *Nature* 1998, *395*, 137–143.
82. Vangone, A.; Schaarschmidt, J.; Koukos, P.; Geng, C.; Citro, N.; Trellet, M.E.; Xue, L.C.; Bonvin, A.M.J.J. Large-scale prediction of binding affinity in protein-small ligand complexes: the PRODIGY-LIG web server. *Bioinformatics* 2019, *35*, 1585–1587.
83. Ferdowsian, H.R., Beck, N. Ethical and scientific considerations regarding animal testing and research. *PLoS One* 2011, *6*, e24059.
84. Morton D.B. Humane endpoints in animal experimentation for biomedical research: ethical, legal and practical aspects. 1998; pp:5-12.
85. The ARRIVE guidelines 2.0. ARRIVE Essential 10. Available on: <https://arriveguidelines.org/arrive-guidelines> (accessed on January 5, 2023).
86. Maheshwari, R.A., Parmar, G.R., Hinsu, D., Seth, A.K., Balaraman, R. Novel therapeutic intervention of coenzyme Q10 and its combination with pioglitazone on the mRNA expression level of adipocytokines in diabetic rats. *Life Sci.* 2020, *258*, 118155.

**Disclaimer/Publisher's Note:** The statements, opinions and data contained in all publications are solely those of the individual author(s) and contributor(s) and not of MDPI and/or the editor(s). MDPI and/or the editor(s) disclaim responsibility for any injury to people or property resulting from any ideas, methods, instructions or products referred to in the content.